

Inclusive Search for Squark and Gluino Production in $p\bar{p}$ Collisions at $\sqrt{s} = 1.96$ TeV

T. Aaltonen,²⁴ J. Adelman,¹⁴ T. Akimoto,⁵⁶ M.G. Albrow,¹⁸ B. Álvarez González,¹² S. Amerio^{x,44} D. Amidei,³⁵
A. Anastassov,³⁹ A. Annovi,²⁰ J. Antos,¹⁵ G. Apollinari,¹⁸ A. Apresyan,⁴⁹ T. Arisawa,⁵⁸ A. Artikov,¹⁶
W. Ashmanskas,¹⁸ A. Attal,⁴ A. Aurisano,⁵⁴ F. Azfar,⁴³ P. Azzurri^{aa,47} W. Badgett,¹⁸ A. Barbaro-Galtieri,²⁹
V.E. Barnes,⁴⁹ B.A. Barnett,²⁶ V. Bartsch,³¹ G. Bauer,³³ P.-H. Beauchemin,³⁴ F. Bedeschi,⁴⁷ D. Beecher,³¹
S. Behari,²⁶ G. Bellettini^{y,47} J. Bellinger,⁶⁰ D. Benjamin,¹⁷ A. Beretvas,¹⁸ J. Beringer,²⁹ A. Bhatti,⁵¹ M. Binkley,¹⁸
D. Bisello^{x,44} I. Bizjak^{dd,31} R.E. Blair,² C. Blocker,⁷ B. Blumenfeld,²⁶ A. Bocci,¹⁷ A. Bodek,⁵⁰ V. Boisvert,⁵⁰
G. Bolla,⁴⁹ D. Bortoletto,⁴⁹ J. Boudreau,⁴⁸ A. Boveia,¹¹ B. Brau^{a,11} A. Bridgeman,²⁵ L. Brigliadori,⁴⁴
C. Bromberg,³⁶ E. Brubaker,¹⁴ J. Budagov,¹⁶ H.S. Budd,⁵⁰ S. Budd,²⁵ S. Burke,¹⁸ K. Burkett,¹⁸ G. Busetto^{x,44}
P. Bussey^{k,22} A. Buzatu,³⁴ K. L. Byrum,² S. Cabrera^{u,17} C. Calancha,³² M. Campanelli,³⁶ M. Campbell,³⁵
F. Canelli,¹⁸ A. Canepa,⁴⁶ B. Carls,²⁵ D. Carlsmith,⁶⁰ R. Carosi,⁴⁷ S. Carrillo^{m,19} S. Carron,³⁴ B. Casal,¹²
M. Casarsa,¹⁸ A. Castro^{w,6} P. Catastini^{z,47} D. Cauz^{cc,55} V. Cavaliere^{z,47} M. Cavalli-Sforza,⁴ A. Cerri,²⁹
L. Cerrito^{n,31} S.H. Chang,²⁸ Y.C. Chen,¹ M. Chertok,⁸ G. Chiarelli,⁴⁷ G. Chlachidze,¹⁸ F. Chlebana,¹⁸ K. Cho,²⁸
D. Chokheli,¹⁶ J.P. Chou,²³ G. Choudalakis,³³ S.H. Chuang,⁵³ K. Chung,¹³ W.H. Chung,⁶⁰ Y.S. Chung,⁵⁰
T. Chwalek,²⁷ C.I. Ciobanu,⁴⁵ M.A. Ciocci^{z,47} A. Clark,²¹ D. Clark,⁷ G. Compostella,⁴⁴ M.E. Convery,¹⁸
J. Conway,⁸ M. Cordelli,²⁰ G. Cortiana^{x,44} C.A. Cox,⁸ D.J. Cox,⁸ F. Crescioli^{y,47} C. Cuenca Almenar^{u,8}
J. Cuevas^{r,12} R. Culbertson,¹⁸ J.C. Cully,³⁵ D. Dagenhart,¹⁸ M. Datta,¹⁸ T. Davies,²² P. de Barbaro,⁵⁰
S. De Cecco,⁵² A. Deisher,²⁹ G. De Lorenzo,⁴ M. Dell'Orso^{y,47} C. Deluca,⁴ L. Demortier,⁵¹ J. Deng,¹⁷ M. Deninno,⁶
P.F. Derwent,¹⁸ G.P. di Giovanni,⁴⁵ C. Dionisi^{bb,52} B. Di Ruzza^{cc,55} J.R. Dittmann,⁵ M. D'Onofrio,⁴ S. Donati^{y,47}
P. Dong,⁹ J. Donini,⁴⁴ T. Dorigo,⁴⁴ S. Dube,⁵³ J. Efron,⁴⁰ A. Elagin,⁵⁴ R. Erbacher,⁸ D. Errede,²⁵ S. Errede,²⁵
R. Eusebi,¹⁸ H.C. Fang,²⁹ S. Farrington,⁴³ W.T. Fedorko,¹⁴ R.G. Feild,⁶¹ M. Feindt,²⁷ J.P. Fernandez,³²
C. Ferrazza^{aa,47} R. Field,¹⁹ G. Flanagan,⁴⁹ R. Forrest,⁸ M.J. Frank,⁵ M. Franklin,²³ J.C. Freeman,¹⁸ I. Furic,¹⁹
M. Gallinaro,⁵² J. Galyardt,¹³ F. Garbersson,¹¹ J.E. Garcia,²¹ A.F. Garfinkel,⁴⁹ K. Genser,¹⁸ H. Gerberich,²⁵
D. Gerdes,³⁵ A. Gessler,²⁷ S. Giagu^{bb,52} V. Giakoumopoulou,³ P. Giannetti,⁴⁷ K. Gibson,⁴⁸ J.L. Gimmell,⁵⁰
C.M. Ginsburg,¹⁸ N. Giokaris,³ M. Giordani^{cc,55} P. Giromini,²⁰ M. Giunta^{y,47} G. Giurgiu,²⁶ V. Glagolev,¹⁶
D. Glenzinski,¹⁸ M. Gold,³⁸ N. Goldschmidt,¹⁹ A. Golossanov,¹⁸ G. Gomez,¹² G. Gomez-Ceballos,³³
M. Goncharov,⁵⁴ O. González,³² I. Gorelov,³⁸ A.T. Goshaw,¹⁷ K. Goulianos,⁵¹ A. Gresele^{x,44} S. Grinstein,²³
C. Grosso-Pilcher,¹⁴ R.C. Group,¹⁸ U. Grundler,²⁵ J. Guimaraes da Costa,²³ Z. Gunay-Unalan,³⁶ C. Haber,²⁹
K. Hahn,³³ S.R. Hahn,¹⁸ E. Halkiadakis,⁵³ B.-Y. Han,⁵⁰ J.Y. Han,⁵⁰ F. Happacher,²⁰ K. Hara,⁵⁶ D. Hare,⁵³
M. Hare,⁵⁷ S. Harper,⁴³ R.F. Harr,⁵⁹ R.M. Harris,¹⁸ M. Hartz,⁴⁸ K. Hatakeyama,⁵¹ C. Hays,⁴³ M. Heck,²⁷
A. Heijboer,⁴⁶ J. Heinrich,⁴⁶ C. Henderson,³³ M. Herndon,⁶⁰ J. Heuser,²⁷ S. Hewamanage,⁵ D. Hidas,¹⁷
C.S. Hill^{c,11} D. Hirschbuehl,²⁷ A. Hocker,¹⁸ S. Hou,¹ M. Houlden,³⁰ S.-C. Hsu,²⁹ B.T. Huffman,⁴³ R.E. Hughes,⁴⁰
U. Husemann,⁶¹ J. Huston,³⁶ J. Incandela,¹¹ G. Introzzi,⁴⁷ M. Iori^{bb,52} A. Ivanov,⁸ E. James,¹⁸ B. Jayatilaka,¹⁷
E.J. Jeon,²⁸ M.K. Jha,⁶ S. Jindariani,¹⁸ W. Johnson,⁸ M. Jones,⁴⁹ K.K. Joo,²⁸ S.Y. Jun,¹³ J.E. Jung,²⁸
T.R. Junk,¹⁸ T. Kamon,⁵⁴ D. Kar,¹⁹ P.E. Karchin,⁵⁹ Y. Kato,⁴² R. Kephart,¹⁸ J. Keung,⁴⁶ V. Khotilovich,⁵⁴
B. Kilminster,¹⁸ D.H. Kim,²⁸ H.S. Kim,²⁸ H.W. Kim,²⁸ J.E. Kim,²⁸ M.J. Kim,²⁰ S.B. Kim,²⁸ S.H. Kim,⁵⁶
Y.K. Kim,¹⁴ N. Kimura,⁵⁶ L. Kirsch,⁷ S. Klimenko,¹⁹ B. Knuteson,³³ B.R. Ko,¹⁷ K. Kondo,⁵⁸ D.J. Kong,²⁸
J. Konigsberg,¹⁹ A. Korytov,¹⁹ A.V. Kotwal,¹⁷ M. Kreps,²⁷ J. Kroll,⁴⁶ D. Krop,¹⁴ N. Krumnack,⁵ M. Kruse,¹⁷
V. Krutelyov,¹¹ T. Kubo,⁵⁶ T. Kuhr,²⁷ N.P. Kulkarni,⁵⁹ M. Kurata,⁵⁶ Y. Kusakabe,⁵⁸ S. Kwang,¹⁴ A.T. Laasanen,⁴⁹
S. Lami,⁴⁷ S. Lammel,¹⁸ M. Lancaster,³¹ R.L. Lander,⁸ K. Lannon^{q,40} A. Lath,⁵³ G. Latino^{z,47} I. Lazzizzera^{x,44}
T. LeCompte,² E. Lee,⁵⁴ H.S. Lee,¹⁴ S.W. Lee^{t,54} S. Leone,⁴⁷ J.D. Lewis,¹⁸ C.-S. Lin,²⁹ J. Linacre,⁴³ M. Lindgren,¹⁸
E. Lipeles,⁴⁶ A. Lister,⁸ D.O. Litvintsev,¹⁸ C. Liu,⁴⁸ T. Liu,¹⁸ N.S. Lockyer,⁴⁶ A. Loginov,⁶¹ M. Loretix^{x,44}
L. Lovas,¹⁵ D. Lucchesi^{x,44} C. Luci^{bb,52} J. Lueck,²⁷ P. Lujan,²⁹ P. Lukens,¹⁸ G. Lungu,⁵¹ L. Lyons,⁴³ J. Lys,²⁹
R. Lysak,¹⁵ D. MacQueen,³⁴ R. Madrak,¹⁸ K. Maeshima,¹⁸ K. Makhoul,³³ T. Maki,²⁴ P. Maksimovic,²⁶ S. Malde,⁴³
S. Malik,³¹ G. Manca^{e,30} A. Manousakis-Katsikakis,³ F. Margaroli,⁴⁹ C. Marino,²⁷ C.P. Marino,²⁵ A. Martin,⁶¹
V. Martin^{l,22} M. Martínez,⁴ R. Martínez-Ballarín,³² T. Maruyama,⁵⁶ P. Mastrandrea,⁵² T. Masubuchi,⁵⁶
M. Mathis,²⁶ M.E. Mattson,⁵⁹ P. Mazzanti,⁶ K.S. McFarland,⁵⁰ P. McIntyre,⁵⁴ R. McNulty^{j,30} A. Mehta,³⁰
P. Mehtala,²⁴ A. Menzione,⁴⁷ P. Merkel,⁴⁹ C. Mesropian,⁵¹ T. Miao,¹⁸ N. Miladinovic,⁷ R. Miller,³⁶ C. Mills,²³
M. Milnik,²⁷ A. Mitra,¹ G. Mitselmakher,¹⁹ H. Miyake,⁵⁶ N. Moggi,⁶ C.S. Moon,²⁸ R. Moore,¹⁸ M.J. Morello^{y,47}
J. Morlok,²⁷ P. Movilla Fernandez,¹⁸ J. Mülmenstädt,²⁹ A. Mukherjee,¹⁸ Th. Muller,²⁷ R. Mumford,²⁶ P. Murat,¹⁸
M. Mussini^{w,6} J. Nachtman,¹⁸ Y. Nagai,⁵⁶ A. Nagano,⁵⁶ J. Naganoma,⁵⁶ K. Nakamura,⁵⁶ I. Nakano,⁴¹ A. Napier,⁵⁷

V. Nacula,¹⁷ J. Nett,⁶⁰ C. Neu^v,⁴⁶ M.S. Neubauer,²⁵ S. Neubauer,²⁷ J. Nielsen^g,²⁹ L. Nodulman,² M. Norman,¹⁰ O. Norriella,²⁵ E. Nurse,³¹ L. Oakes,⁴³ S.H. Oh,¹⁷ Y.D. Oh,²⁸ I. Oksuzian,¹⁹ T. Okusawa,⁴² R. Orava,²⁴ S. Pagan Griso^x,⁴⁴ E. Palencia,¹⁸ V. Papadimitriou,¹⁸ A. Papaikonomou,²⁷ A.A. Paramonov,¹⁴ B. Parks,⁴⁰ S. Pashapour,³⁴ J. Patrick,¹⁸ G. Pauletta^{cc},⁵⁵ M. Paulini,¹³ C. Paus,³³ T. Peiffer,²⁷ D.E. Pellett,⁸ A. Penzo,⁵⁵ T.J. Phillips,¹⁷ G. Piacentino,⁴⁷ E. Pianori,⁴⁶ L. Pinera,¹⁹ K. Pitts,²⁵ C. Plager,⁹ L. Pondrom,⁶⁰ X. Portell^{ee},⁴ O. Poukhov^{*},¹⁶ N. Pounder,⁴³ F. Prakoshyn,¹⁶ A. Pronko,¹⁸ J. Proudfoot,² F. Ptohosⁱ,¹⁸ E. Pueschel,¹³ G. Punzi^y,⁴⁷ J. Pursley,⁶⁰ J. Rademacker^c,⁴³ A. Rahaman,⁴⁸ V. Ramakrishnan,⁶⁰ N. Ranjan,⁴⁹ I. Redondo,³² V. Rekovic,³⁸ P. Renton,⁴³ M. Renz,²⁷ M. Rescigno,⁵² S. Richter,²⁷ F. Rimondi^w,⁶ L. Ristori,⁴⁷ A. Robson,²² T. Rodrigo,¹² T. Rodriguez,⁴⁶ E. Rogers,²⁵ S. Rolli,⁵⁷ R. Roser,¹⁸ M. Rossi,⁵⁵ R. Rossin,¹¹ P. Roy,³⁴ A. Ruiz,¹² J. Russ,¹³ V. Rusu,¹⁸ A. Safonov,⁵⁴ W.K. Sakumoto,⁵⁰ O. Saltó,⁴ L. Santi^{cc},⁵⁵ S. Sarkar^{bb},⁵² L. Sartori,⁴⁷ K. Sato,¹⁸ A. Savoy-Navarro,⁴⁵ P. Schlabach,¹⁸ A. Schmidt,²⁷ E.E. Schmidt,¹⁸ M.A. Schmidt,¹⁴ M.P. Schmidt^{*},⁶¹ M. Schmitt,³⁹ T. Schwarz,⁸ L. Scodellaro,¹² A. Scribano^z,⁴⁷ F. Scuri,⁴⁷ A. Sedov,⁴⁹ S. Seidel,³⁸ Y. Seiya,⁴² A. Semenov,¹⁶ L. Sexton-Kennedy,¹⁸ F. Sforza,⁴⁷ A. Sfyrila,²⁵ S.Z. Shalhout,⁵⁹ T. Shears,³⁰ P.F. Shepard,⁴⁸ M. Shimojima^p,⁵⁶ S. Shiraishi,¹⁴ M. Shochet,¹⁴ Y. Shon,⁶⁰ I. Shreyber,³⁷ A. Sidoti,⁴⁷ P. Sinervo,³⁴ A. Sisakyan,¹⁶ A.J. Slaughter,¹⁸ J. Slaunwhite,⁴⁰ K. Sliwa,⁵⁷ J.R. Smith,⁸ F.D. Snider,¹⁸ R. Snihur,³⁴ A. Soha,⁸ S. Somalwar,⁵³ V. Sorin,³⁶ J. Spalding,¹⁸ T. Spreitzer,³⁴ P. Squillacioti^z,⁴⁷ M. Stanitzki,⁶¹ R. St. Denis,²² B. Stelzer^s,⁹ O. Stelzer-Chilton,¹⁷ D. Stentz,³⁹ J. Strologas,³⁸ G.L. Strycker,³⁵ D. Stuart,¹¹ J.S. Suh,²⁸ A. Sukhanov,¹⁹ I. Suslov,¹⁶ T. Suzuki,⁵⁶ A. Taffard^f,²⁵ R. Takashima,⁴¹ Y. Takeuchi,⁵⁶ R. Tanaka,⁴¹ M. Tecchio,³⁵ P.K. Teng,¹ K. Terashi,⁵¹ J. Thom^h,¹⁸ A.S. Thompson,²² G.A. Thompson,²⁵ E. Thomson,⁴⁶ P. Tipton,⁶¹ P. Ttito-Guzmán,³² S. Tkaczyk,¹⁸ D. Toback,⁵⁴ S. Tokar,¹⁵ K. Tollefson,³⁶ T. Tomura,⁵⁶ D. Tonelli,¹⁸ S. Torre,²⁰ D. Torretta,¹⁸ P. Totaro^{cc},⁵⁵ S. Tourneur,⁴⁵ M. Trovato,⁴⁷ S.-Y. Tsai,¹ Y. Tu,⁴⁶ N. Turini^z,⁴⁷ F. Ukegawa,⁵⁶ S. Vallecorsa,²¹ N. van Remortel^b,²⁴ A. Varganov,³⁵ E. Vataga^{aa},⁴⁷ F. Vázquez^m,¹⁹ G. Velev,¹⁸ C. Vellidis,³ V. Veszpremi,⁴⁹ M. Vidal,³² R. Vidal,¹⁸ I. Vila,¹² R. Vilar,¹² T. Vine,³¹ M. Vogel,³⁸ I. Volobouev^t,²⁹ G. Volpi^y,⁴⁷ P. Wagner,⁴⁶ R.G. Wagner,² R.L. Wagner,¹⁸ W. Wagner,²⁷ J. Wagner-Kuhr,²⁷ T. Wakisaka,⁴² R. Wallny,⁹ S.M. Wang,¹ A. Warburton,³⁴ D. Waters,³¹ M. Weinberger,⁵⁴ J. Weinelt,²⁷ W.C. Wester III,¹⁸ B. Whitehouse,⁵⁷ D. Whiteson^f,⁴⁶ A.B. Wicklund,² E. Wicklund,¹⁸ S. Wilbur,¹⁴ G. Williams,³⁴ H.H. Williams,⁴⁶ P. Wilson,¹⁸ B.L. Winer,⁴⁰ P. Wittich^h,¹⁸ S. Wolbers,¹⁸ C. Wolfe,¹⁴ T. Wright,³⁵ X. Wu,²¹ F. Würthwein,¹⁰ S.M. Wynne,³⁰ S. Xie,³³ A. Yagil,¹⁰ K. Yamamoto,⁴² J. Yamaoka,⁵³ U.K. Yang^o,¹⁴ Y.C. Yang,²⁸ W.M. Yao,²⁹ G.P. Yeh,¹⁸ J. Yoh,¹⁸ K. Yorita,¹⁴ T. Yoshida,⁴² G.B. Yu,⁵⁰ I. Yu,²⁸ S.S. Yu,¹⁸ J.C. Yun,¹⁸ L. Zanello^{bb},⁵² A. Zanetti,⁵⁵ X. Zhang,²⁵ Y. Zheng^d,⁹ and S. Zucchelli^w,⁶

(CDF Collaboration[†])

¹*Institute of Physics, Academia Sinica, Taipei, Taiwan 11529, Republic of China*

²*Argonne National Laboratory, Argonne, Illinois 60439*

³*University of Athens, 157 71 Athens, Greece*

⁴*Institut de Física d'Altes Energies, Universitat Autònoma de Barcelona, E-08193, Bellaterra (Barcelona), Spain*

⁵*Baylor University, Waco, Texas 76798*

⁶*Istituto Nazionale di Fisica Nucleare Bologna, ^wUniversity of Bologna, I-40127 Bologna, Italy*

⁷*Brandeis University, Waltham, Massachusetts 02254*

⁸*University of California, Davis, Davis, California 95616*

⁹*University of California, Los Angeles, Los Angeles, California 90024*

¹⁰*University of California, San Diego, La Jolla, California 92093*

¹¹*University of California, Santa Barbara, Santa Barbara, California 93106*

¹²*Instituto de Física de Cantabria, CSIC-University of Cantabria, 39005 Santander, Spain*

¹³*Carnegie Mellon University, Pittsburgh, PA 15213*

¹⁴*Enrico Fermi Institute, University of Chicago, Chicago, Illinois 60637*

¹⁵*Comenius University, 842 48 Bratislava, Slovakia; Institute of Experimental Physics, 040 01 Kosice, Slovakia*

¹⁶*Joint Institute for Nuclear Research, RU-141980 Dubna, Russia*

¹⁷*Duke University, Durham, North Carolina 27708*

¹⁸*Fermi National Accelerator Laboratory, Batavia, Illinois 60510*

¹⁹*University of Florida, Gainesville, Florida 32611*

²⁰*Laboratori Nazionali di Frascati, Istituto Nazionale di Fisica Nucleare, I-00044 Frascati, Italy*

²¹*University of Geneva, CH-1211 Geneva 4, Switzerland*

²²*Glasgow University, Glasgow G12 8QQ, United Kingdom*

²³*Harvard University, Cambridge, Massachusetts 02138*

²⁴*Division of High Energy Physics, Department of Physics, University of Helsinki and Helsinki Institute of Physics, FIN-00014, Helsinki, Finland*

²⁵*University of Illinois, Urbana, Illinois 61801*

- ²⁶The Johns Hopkins University, Baltimore, Maryland 21218
- ²⁷Institut für Experimentelle Kernphysik, Universität Karlsruhe, 76128 Karlsruhe, Germany
- ²⁸Center for High Energy Physics: Kyungpook National University, Daegu 702-701, Korea; Seoul National University, Seoul 151-742, Korea; Sungkyunkwan University, Suwon 440-746, Korea; Korea Institute of Science and Technology Information, Daejeon, 305-806, Korea; Chonnam National University, Gwangju, 500-757, Korea
- ²⁹Ernest Orlando Lawrence Berkeley National Laboratory, Berkeley, California 94720
- ³⁰University of Liverpool, Liverpool L69 7ZE, United Kingdom
- ³¹University College London, London WC1E 6BT, United Kingdom
- ³²Centro de Investigaciones Energeticas Medioambientales y Tecnologicas, E-28040 Madrid, Spain
- ³³Massachusetts Institute of Technology, Cambridge, Massachusetts 02139
- ³⁴Institute of Particle Physics: McGill University, Montréal, Canada H3A 2T8; and University of Toronto, Toronto, Canada M5S 1A7
- ³⁵University of Michigan, Ann Arbor, Michigan 48109
- ³⁶Michigan State University, East Lansing, Michigan 48824
- ³⁷Institution for Theoretical and Experimental Physics, ITEP, Moscow 117259, Russia
- ³⁸University of New Mexico, Albuquerque, New Mexico 87131
- ³⁹Northwestern University, Evanston, Illinois 60208
- ⁴⁰The Ohio State University, Columbus, Ohio 43210
- ⁴¹Okayama University, Okayama 700-8530, Japan
- ⁴²Osaka City University, Osaka 588, Japan
- ⁴³University of Oxford, Oxford OX1 3RH, United Kingdom
- ⁴⁴Istituto Nazionale di Fisica Nucleare, Sezione di Padova-Trento, ^xUniversity of Padova, I-35131 Padova, Italy
- ⁴⁵LPNHE, Universite Pierre et Marie Curie/IN2P3-CNRS, UMR7585, Paris, F-75252 France
- ⁴⁶University of Pennsylvania, Philadelphia, Pennsylvania 19104
- ⁴⁷Istituto Nazionale di Fisica Nucleare Pisa, ^yUniversity of Pisa, ^zUniversity of Siena and ^{aa}Scuola Normale Superiore, I-56127 Pisa, Italy
- ⁴⁸University of Pittsburgh, Pittsburgh, Pennsylvania 15260
- ⁴⁹Purdue University, West Lafayette, Indiana 47907
- ⁵⁰University of Rochester, Rochester, New York 14627
- ⁵¹The Rockefeller University, New York, New York 10021
- ⁵²Istituto Nazionale di Fisica Nucleare, Sezione di Roma 1, ^{bb}Sapienza Università di Roma, I-00185 Roma, Italy
- ⁵³Rutgers University, Piscataway, New Jersey 08855
- ⁵⁴Texas A&M University, College Station, Texas 77843
- ⁵⁵Istituto Nazionale di Fisica Nucleare Trieste/Udine, ^{cc}University of Trieste/Udine, Italy
- ⁵⁶University of Tsukuba, Tsukuba, Ibaraki 305, Japan
- ⁵⁷Tufts University, Medford, Massachusetts 02155
- ⁵⁸Waseda University, Tokyo 169, Japan
- ⁵⁹Wayne State University, Detroit, Michigan 48201
- ⁶⁰University of Wisconsin, Madison, Wisconsin 53706
- ⁶¹Yale University, New Haven, Connecticut 06520
- (Dated: October 20, 2009)

We report on a search for inclusive production of squarks and gluinos in $p\bar{p}$ collisions at $\sqrt{s} = 1.96$ TeV, in events with large missing transverse energy and multiple jets of hadrons in the final state. The study uses a CDF Run II data sample corresponding to 2 fb^{-1} of integrated luminosity. The data are in good agreement with the standard model predictions, giving no evidence for any squark or gluino component. In an R-parity conserving minimal supergravity scenario with $A_0 = 0$, $\mu < 0$ and $\tan\beta = 5$, 95% C.L. upper limits on the production cross sections in the range between 0.1 pb and 1 pb are obtained, depending on the squark and gluino masses considered. For gluino masses below $280 \text{ GeV}/c^2$, arbitrarily large squark masses are excluded at the 95% C.L., while for mass degenerate gluinos and squarks, masses below $392 \text{ GeV}/c^2$ are excluded at the 95% C.L.

PACS numbers: 14.80.Ly, 12.60.Jv

*Deceased

†With visitors from ^aUniversity of Massachusetts Amherst, Amherst, Massachusetts 01003, ^bUniversiteit Antwerpen, B-2610

Antwerp, Belgium, ^cUniversity of Bristol, Bristol BS8 1TL, United Kingdom, ^dChinese Academy of Sciences, Beijing 100864, China, ^eIstituto Nazionale di Fisica Nucleare, Sezione di Cagliari,

Supersymmetry (SUSY) [1] is regarded as a possible extension of the standard model (SM) that naturally solves the hierarchy problem and provides a possible candidate for dark matter in the Universe. SUSY introduces a new symmetry that relates fermionic and bosonic degrees of freedom, and doubles the SM spectrum of particles by introducing a new supersymmetric partner (sparticle) for each particle in the SM. Results on similar inclusive searches for SUSY using Tevatron data have been previously reported by both the CDF and D0 experiments in Run I [2] and by the D0 experiment in Run II [3]. This Letter presents new results on an inclusive search for squarks and gluinos, supersymmetric partners of quarks and gluons, based on data collected by the CDF experiment in Run II and corresponding to 2.0 fb^{-1} of integrated luminosity. The analysis is performed within the framework of minimal supergravity (mSUGRA) [4] and assumes R-parity conservation where sparticles are produced in pairs and the lightest supersymmetric particle (LSP) is stable, neutral, and weakly interacting. The expected signal is characterized by the production of multiple jets of hadrons from the cascade decays of squarks and gluinos and large missing transverse energy \cancel{E}_T [5] from the presence of two LSPs in the final state. In a scenario with squark masses $M_{\tilde{q}}$ significantly larger than the gluino mass $M_{\tilde{g}}$ at least four jets in the final state are expected, while for $M_{\tilde{g}} > M_{\tilde{q}}$ dijet configurations dominate. Separate analyses are carried out for events with at least two, three, and four jets in the final state and with different requirements on the minimum \cancel{E}_T . The results are compared to SM background predictions from quantum chromodynamics (QCD) jets, W and Z/γ^* bosons with accompanying jets (W +jets and Z/γ^* +jets), top quark, and diboson (WW , ZW and ZZ) processes.

The CDF II detector is described in detail elsewhere [6]. The detector has a charged particle tracking system that is immersed in a 1.4 T solenoidal magnetic field coaxial with the beam line, and provides coverage in

the pseudorapidity [5] range $|\eta| \leq 2$. Segmented sampling calorimeters, arranged in a projective tower geometry, surround the tracking system and measure the energy of interacting particles for $|\eta| < 3.6$. The central electromagnetic and hadronic calorimeters cover the region $|\eta| < 1$, while the endwall hadronic calorimeter provides coverage out to $|\eta| < 1.3$. Forward electromagnetic and hadronic calorimeters cover the regions $1.1 < |\eta| < 3.6$ and $1.3 < |\eta| < 3.6$, respectively. Cherenkov counters in the region $3.7 < |\eta| < 4.7$ measure the number of inelastic $p\bar{p}$ collisions to determine the luminosity [7].

Simulated event samples are used to determine detector acceptance and reconstruction efficiency, estimate SM background contributions, and compute the number of expected SUSY signal events. Samples of simulated QCD-jets, $t\bar{t}$ production, and diboson processes are generated using the PYTHIA 6.216 [8] Monte Carlo generator with Tune A [9]. The normalization of the QCD-jets sample is extracted from data in a low \cancel{E}_T region, while $t\bar{t}$ and diboson samples are normalized to next-to-leading order (NLO) predictions [10, 11]. Samples of simulated Z/γ^* +jets and W +jets events are generated using the ALPGEN 2.1 program [12] where exclusive subsamples with different jet multiplicities are combined, and the resulting samples are normalized to the measured Z and W inclusive cross sections [13]. Finally, samples of single top events are produced using the MADEVENT program [14] and normalized using NLO predictions [15]. In mSUGRA, the mass spectrum of sparticles is determined by five parameters: the common scalar and gaugino masses at the GUT scale, M_0 and $M_{1/2}$, respectively; the common trilinear coupling at the GUT scale, A_0 ; the sign of the Higgsino mixing parameter, μ ; and the ratio of the Higgs vacuum expectation values, $\tan\beta$. The mSUGRA samples are generated using the ISASUGRA implementation in PYTHIA with $A_0 = 0$, $\mu < 0$, and $\tan\beta = 5$, as inspired by previous studies [16]. A total of 132 different squark and gluino masses are generated via variations of M_0 and $M_{1/2}$ in the range $M_0 < 600 \text{ GeV}/c^2$ and $50 < M_{1/2} < 220 \text{ GeV}/c^2$. At low $\tan\beta$, the squarks from the first two generations are nearly degenerate, whereas the mixing of the third generation leads to slightly lighter sbottom masses and much lighter stop masses. In this analysis, stop pair production processes are not considered. The contribution from hard processes involving sbottom production is almost negligible, and is not included in the calculation of the signal efficiencies to avoid a dependency on the details of the model for squark mixing. The mSUGRA samples are normalized using NLO cross sections as determined by PROSPINO 2.0 [17], with input parameters provided by ISAJET 7.74 [18]. CTEQ61M parton distribution functions (PDFs) [19] are used, and renormalization and factorization scales are set to the average mass [20] of the sparticles produced in the hard interaction. The Monte Carlo events are passed through a full CDF II detector

09042 Monserrato (Cagliari), Italy, ^fUniversity of California Irvine, Irvine, CA 92697, ^gUniversity of California Santa Cruz, Santa Cruz, CA 95064, ^hCornell University, Ithaca, NY 14853, ⁱUniversity of Cyprus, Nicosia CY-1678, Cyprus, ^jUniversity College Dublin, Dublin 4, Ireland, ^kRoyal Society of Edinburgh/Scottish Executive Support Research Fellow, ^lUniversity of Edinburgh, Edinburgh EH9 3JZ, United Kingdom, ^mUniversidad Iberoamericana, Mexico D.F., Mexico, ⁿQueen Mary, University of London, London, E1 4NS, England, ^oUniversity of Manchester, Manchester M13 9PL, England, ^pNagasaki Institute of Applied Science, Nagasaki, Japan, ^qUniversity of Notre Dame, Notre Dame, IN 46556, ^rUniversity de Oviedo, E-33007 Oviedo, Spain, ^sSimon Fraser University, Vancouver, British Columbia, Canada V6B 5K3, ^tTexas Tech University, Lubbock, TX 79409, ^uIFIC(CSIC-Universitat de Valencia), 46071 Valencia, Spain, ^vUniversity of Virginia, Charlottesville, VA 22904, ^{dd}On leave from J. Stefan Institute, Ljubljana, Slovenia, ^{ee}Now at Freiburg University, Germany,

simulation (based on GEANT3 [21] and GFLASH [22]) and reconstructed and analyzed with the same analysis chain as for the data.

Data are collected using a three-level trigger system that selects events with $\cancel{E}_T > 35$ GeV and at least two calorimeter clusters with E_T above 10 GeV. The events are then required to have a primary vertex with a z position within 60 cm of the nominal interaction. Jets are reconstructed from the energy deposits in the calorimeter towers using a cone-based jet algorithm [23] with cone radius $R = \sqrt{\Delta\eta^2 + \Delta\phi^2} = 0.7$, and the measured E_T^{jet} is corrected for detector effects and contributions from multiple $p\bar{p}$ interactions per crossing at high instantaneous luminosity, as discussed in Ref. [24]. The events are required to have at least two, three, or four jets (depending on the final state considered), each jet with corrected transverse energy $E_T^{\text{jet}} > 25$ GeV and pseudorapidity in the range $|\eta^{\text{jet}}| < 2.0$, and at least one of the jets is required to have $|\eta^{\text{jet}}| < 1.1$. Finally, the events are required to have $\cancel{E}_T > 70$ GeV. For the kinematic range in \cancel{E}_T and the E_T^{jet} of the jets considered in this analysis, the trigger selection is 100% efficient. Beam-related backgrounds and cosmic rays are removed by requiring an average jet electromagnetic fraction $f_{\text{em}} = \sum_{\text{jets}} E_{T,\text{em}}^{\text{jet}} / \sum_{\text{jets}} E_T^{\text{jet}} > 0.15$, where $E_{T,\text{em}}^{\text{jet}}$ denotes the electromagnetic component of the jet transverse energy, and the sums run over all the selected jets in the event. In addition, the events are required to have an average charged particle fraction $f_{\text{ch}} = \sum_{\text{jets}} p_{T,\text{trk}}^{\text{jet}} / \sum_{\text{jets}} E_T^{\text{jet}} > 0.15$, where, for each selected jet with $|\eta^{\text{jet}}| < 1.1$, $p_{T,\text{trk}}^{\text{jet}}$ is computed as the scalar sum of the transverse momenta p_T^{track} of tracks with $p_T^{\text{track}} > 0.3$ GeV/ c and within a cone of radius $R = 0.4$ around the jet axis. The requirements on f_{em} and f_{ch} reject events with anomalous energy deposition in the hadronic section of the calorimeter or energy deposits in the calorimeter inconsistent with the observed activity in the tracking system, and have no significant effect on the mSUGRA and SM Monte Carlo samples.

The dominant QCD-jets background with large \cancel{E}_T originates from the misreconstruction of the jet energies in the calorimeters. In such events the \cancel{E}_T direction tends to be aligned, in the transverse plane, with one of the leading jets in the event. This background contribution is suppressed by requiring an azimuthal separation $\Delta\phi(\cancel{E}_T - \text{jet}) > 0.7$ for each of the selected jets in the event. In the case of the four-jets analysis, the requirement for the least energetic jet is limited to $\Delta\phi(\cancel{E}_T - \text{jet}) > 0.3$. Finally, in the two-jets analysis case the events are rejected if they contain a third jet with $E_T^{\text{jet}} > 25$ GeV, $|\eta^{\text{jet}}| < 2.0$, and $\Delta\phi(\cancel{E}_T - \text{jet}) < 0.2$. The SM background contributions with energetic electrons [25] in the final state from Z and W decays are suppressed by requiring $E_{T,\text{em}}^{\text{jet}}/E_T^{\text{jet}} < 0.9$ for each selected jet in the event. In addition, events

that have one isolated track with $p_T^{\text{track}} > 10$ GeV/ c and $\Delta\phi(\cancel{E}_T - \text{track}) < 0.7$, or two isolated tracks with an invariant mass $76 < M_{\text{trks}} < 106$ GeV/ c^2 , are vetoed to reject backgrounds with W or Z bosons decaying into muon or tau leptons.

An optimization is carried out to determine, for each final state, the lower thresholds on \cancel{E}_T , the E_T^{jet} of the individual jets, and H_T , defined as $H_T = \sum_{\text{jets}} E_T^{\text{jet}}$ [26]. For each mSUGRA sample, the procedure maximizes S/\sqrt{B} , where S denotes the number of SUSY events and B is the total SM background. The results from the different mSUGRA samples are then combined to define, for each final state, a single set of lower thresholds that maximizes the search sensitivity in the widest range of squark and gluino masses (see Table I). As an example, for $M_{\tilde{q}} = M_{\tilde{g}}$ and masses between 300 GeV/ c^2 and 400 GeV/ c^2 , values for S/\sqrt{B} in the range between 20 and 6 are obtained, corresponding to SUSY selection efficiencies of 4% to 12%, respectively.

Lower thresholds (GeV)						
Final state	\cancel{E}_T	H_T	$E_T^{\text{jet}(1)}$	$E_T^{\text{jet}(2)}$	$E_T^{\text{jet}(3)}$	$E_T^{\text{jet}(4)}$
$\cancel{E}_T + \geq 2$ jets	180	330	165	100	-	-
$\cancel{E}_T + \geq 3$ jets	120	330	140	100	25	-
$\cancel{E}_T + \geq 4$ jets	90	280	95	55	55	25

TABLE I: Optimized lower thresholds on \cancel{E}_T , H_T , and $E_T^{\text{jet}(i)}$ ($i = 1 - 4$) for each analysis.

A number of control samples in data are considered to test the validity of the SM background predictions, as extracted from simulated events. The samples are defined by reversing the logic of some of the selection criteria described above. A sample dominated by QCD jets is obtained by requiring that at least one of the selected jets is aligned with the \cancel{E}_T direction. A control sample dominated by $Z/\gamma^* + \text{jets}$, $W + \text{jets}$, and top-quark processes with highly energetic electrons in the final state is obtained after requiring $E_{T,\text{em}}^{\text{jet}}/E_T^{\text{jet}} > 0.9$ for at least one of the jets. Similarly, a control sample with highly energetic muons in the final state is created by requiring the presence of an isolated track with $p_T^{\text{track}} > 10$ GeV/ c and $\Delta\phi(\cancel{E}_T - \text{track}) < 0.7$, or two isolated tracks with $76 < M_{\text{trks}} < 106$ GeV/ c^2 . Good agreement is observed between the data and the SM predictions in each of the control regions for all the final states considered.

A detailed study of the systematic uncertainties is carried out for each final state [27, 28]. A 3% uncertainty on the absolute jet energy scale [24] in the calorimeter introduces an uncertainty in the background prediction that varies between 24% and 34%, and an uncertainty on the mSUGRA signal efficiencies between 15% and 17%. Uncertainties related to the modeling of the initial- and final-state soft gluon radiation in the simulated samples translate into a 3% to 6% uncertainty on the mSUGRA signal efficiency, and uncertainties on

the background predictions that vary between 8% and 10%. An additional 10% uncertainty on the diboson and top quark contributions accounts for the uncertainty on the predicted cross sections at NLO. A 2% uncertainty on the measured Drell-Yan cross sections, relevant for $Z/\gamma^* + \text{jets}$ and $W + \text{jets}$ processes, is also included. The total systematic uncertainty on the SM predictions varies between 31% and 35% as the jet multiplicity increases. Various sources of uncertainty in the mSUGRA cross sections at NLO, as determined using PROSPINO, are considered. The uncertainty on the PDFs varies between 10% and 20%, depending on the mSUGRA point considered. Variations of the renormalization and factorization scales by a factor of two change the theoretical cross sections by 20% to 25%.

Figure 1 shows the measured H_T and \cancel{E}_T distributions compared to the SM predictions after all final selection criteria are applied. For illustrative purposes, the Figure indicates the impact of a given mSUGRA scenario. The measured distributions are in good agreement with the SM predictions in each of the three final states considered. In Table II, the observed number of events and the SM predictions are presented for each final state. A global χ^2 test, including correlations between systematic uncertainties, gives a 94% probability.

Events in data (2 fb^{-1})			
	$\geq 2 \text{ jets}$	$\geq 3 \text{ jets}$	$\geq 4 \text{ jets}$
	18	38	45
SM predictions			
QCD jets	4.4 ± 2.0	13.3 ± 4.6	15.3 ± 7.1
top	1.3 ± 1.2	7.6 ± 4.1	22.1 ± 7.0
$Z \rightarrow \nu\bar{\nu} + \text{jets}$	3.9 ± 0.9	5.4 ± 1.4	2.7 ± 0.7
$Z/\gamma^* \rightarrow l^+l^- + \text{jets}$	0.1 ± 0.1	0.2 ± 0.1	0.1 ± 0.1
$W \rightarrow l\nu + \text{jets}$	6.1 ± 2.2	10.7 ± 3.1	7.7 ± 2.2
WW, ZW, ZZ	0.2 ± 0.2	0.3 ± 0.2	0.5 ± 0.2
total SM	16 ± 5	37 ± 12	48 ± 17

TABLE II: Number of events in data for each final state compared to SM predictions, including statistical and systematic uncertainties summed in quadrature.

The results are translated into 95% C.L. upper limits on the cross section for squark and gluino production in different regions of the squark-gluino mass plane, using a Bayesian approach [29] and including statistical and systematic uncertainties. For the latter, correlations between systematic uncertainties on signal efficiencies and background predictions are taken into account, and an additional 6% uncertainty on the total luminosity is included. For each mSUGRA point considered, observed and expected limits are computed separately for each of the three analyses, and the one with the best expected limit is adopted as the nominal result. Figure 2 shows the observed and expected 95% C.L. upper limits as a function of squark and gluino masses, compared to mSUGRA predictions, in four regions within the squark-gluino mass

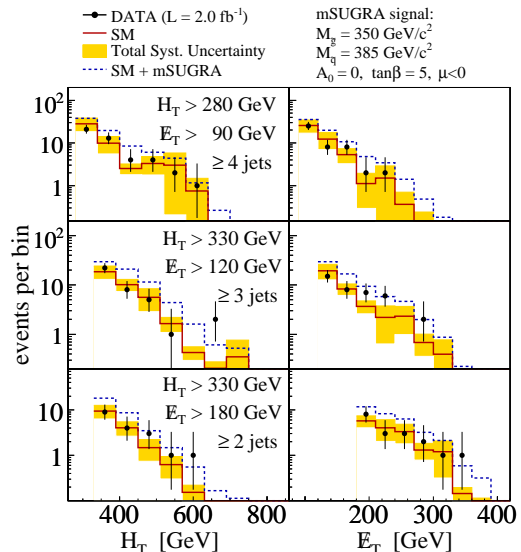


FIG. 1: Measured H_T and \cancel{E}_T distributions (black dots) in events with at least two (bottom), three (middle), and four (top) jets in the final state compared to the SM predictions (solid lines) and the SM+mSUGRA predictions (dashed lines). The shaded bands show the total systematic uncertainty on the SM predictions.

plane. Cross sections in the range between 0.1 pb and 1 pb are excluded by this analysis, depending on the masses considered. The observed numbers of events in data are also translated into 95% C.L. upper limits for squark and gluino masses, for which the uncertainties on the theoretical cross sections are included in the limit calculation, and where the three analyses are combined in a similar way as for the cross section limits. Figure 3 shows the excluded region in the squark-gluino mass plane. For the mSUGRA scenario considered, all squark masses are excluded for $M_{\tilde{g}} < 280 \text{ GeV}/c^2$, while for $M_{\tilde{q}} = M_{\tilde{g}}$ masses up to $392 \text{ GeV}/c^2$ are excluded. Finally, for $M_{\tilde{q}} < 400 \text{ GeV}/c^2$ gluinos with $M_{\tilde{g}} < 340 \text{ GeV}/c^2$ are excluded. This analysis extends the previous Run I limits from the Tevatron by $80 \text{ GeV}/c^2$ to $140 \text{ GeV}/c^2$.

In summary, we report results on an inclusive search for squarks and gluinos in $p\bar{p}$ collisions at $\sqrt{s} = 1.96 \text{ TeV}$ in events with large \cancel{E}_T and multiple jets in the final states, based on 2 fb^{-1} of CDF Run II data. The measurements are in good agreement with SM predictions for backgrounds. The results are translated into 95% C.L. upper limits on production cross sections and squark and gluino masses in a given mSUGRA scenario, which significantly extend Run I results.

We thank the Fermilab staff and the technical staffs of the participating institutions for their vital contributions. This work was supported by the U.S. Department of Energy and National Science Foundation; the Italian Istituto Nazionale di Fisica Nucleare; the Ministry of Education, Culture, Sports, Science and Technology of

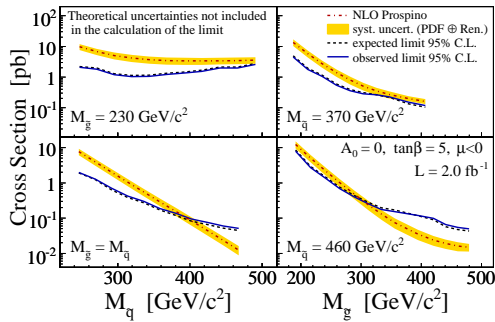


FIG. 2: Observed (solid lines) and expected (dashed lines) 95% C.L. upper limits on the inclusive squark and gluino production cross sections as a function of $M_{\tilde{q}}$ (left) and $M_{\tilde{g}}$ (right) in different regions of the squark-gluino mass plane, compared to NLO mSUGRA predictions (dashed-dotted lines). The shaded bands denote the total uncertainty on the theory.

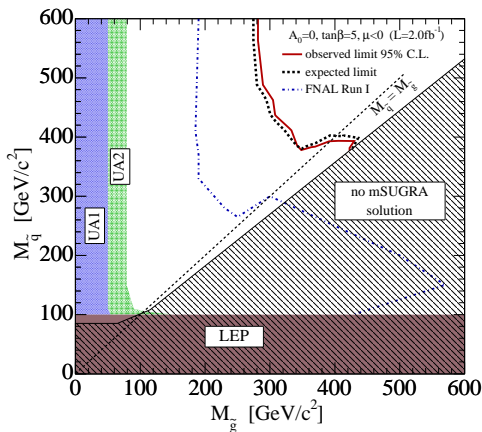


FIG. 3: Exclusion plane at 95 % C.L. as a function of squark and gluino masses in an mSUGRA scenario with $A_0 = 0$, $\mu < 0$ and $\tan\beta = 5$. The observed (solid line) and expected (dashed line) upper limits are compared to previous results from SPS [30] and LEP [31] experiments at CERN (shaded bands), and from the Run I at the Tevatron [2] (dashed-dotted line). The hatched area indicates the region in the plane with no mSUGRA solution.

Japan; the Natural Sciences and Engineering Research Council of Canada; the National Science Council of the Republic of China; the Swiss National Science Foundation; the A.P. Sloan Foundation; the Bundesministerium für Bildung und Forschung, Germany; the Korean Science and Engineering Foundation and the Korean Research Foundation; the Science and Technology Facilities Council and the Royal Society, UK; the Institut National de Physique Nucleaire et Physique des Particules/CNRS; the Russian Foundation for Basic Research; the Ministerio de Ciencia e Innovación, and Programa Consolider-Ingenio 2010, Spain; the Slovak R&D Agency; and the

- [1] H. E. Haber and G. L. Kane, Phys. Rep. **117**, 75 (1985).
- [2] T. Affolder *et al.* (CDF Collaboration), Phys. Rev. Lett. **88**, 041801 (2002); S. Abachi *et al.* (D0 Collaboration), *ibid.* **75**, 618 (1995).
- [3] V.M. Abazov *et al.* (D0 Collaboration), Phys. Lett. B **660**, 449 (2008).
- [4] H. P. Nilles, Phys. Rep. **110**, 1 (1984).
- [5] CDF uses a cylindrical coordinate system about the beam axis with polar angle θ and azimuthal angle ϕ . We define transverse energy $E_T = E \sin\theta$, transverse momentum $p_T = p \sin\theta$, pseudorapidity $\eta = -\ln(\tan(\frac{\theta}{2}))$, and rapidity $y = \frac{1}{2} \ln(\frac{E+p_z}{E-p_z})$. The missing transverse energy \cancel{E}_T is defined as the norm of $-\sum_i E^i \cdot \vec{n}_i$, where \vec{n}_i is the component in the azimuthal plane of the unit vector pointing from the interaction point to the i -th calorimeter tower.
- [6] D. Acosta *et al.* (CDF Collaboration), Phys. Rev. D **71**, 032001 (2005).
- [7] D. Acosta *et al.*, Nucl. Instrum. Methods, A **494**, 57 (2002).
- [8] T. Sjöstrand *et al.*, Comp. Phys. Comm. **135**, 238 (2001).
- [9] T. Affolder *et al.* (CDF Collaboration), Phys. Rev. D **65**, 092002 (2002).
- [10] M. Cacciari *et al.*, J. High Energy Phys. **0404**, 068 (2004).
- [11] J. M. Campbell and R. K. Ellis, Phys. Rev. D **60**, 113006 (1999).
- [12] M.L. Mangano *et al.*, J. High Energy Phys. **07**, 001 (2003).
- [13] A. Abulencia *et al.* (CDF Collaboration), J. Phys. G: Nucl. Part. Phys. **34**, 2457 (2007).
- [14] F. Maltoni and T. Stelzer, J. High Energy Phys. **02**, 027 (2003).
- [15] B. W. Harris *et al.*, Phys. Rev. D **66**, 054024 (2002).
- [16] B. C. Allanach *et al.*, Eur. Phys. J. C **25**, 113 (2002).
- [17] W. Beenakker *et al.*, Nucl. Phys. B **492**, 51 (1997).
- [18] F. Paige and S. Protopopescu, in *Supercollider Physics*, p. 41, ed. D. Soper (World Scientific, 1986).
- [19] J. Pumplin *et al.*, J. High Energy Phys. **0207**, 012 (2002).
- [20] Pole masses are considered. The squark mass is averaged over the first two squark generations.
- [21] R. Brun *et al.*, Tech. Rep. CERN-DD/EE/84-1, 1987.
- [22] G. Grindhammer, M. Rudowicz, and S. Peters, Nucl. Instrum. Methods A **290**, 469 (1990).
- [23] F. Abe *et al.* (CDF Collaboration), Phys. Rev. D **45**, 1448 (1992).
- [24] A. Bhatti *et al.*, Nucl. Instrum. Methods A **566**, 375 (2006).
- [25] Charge conjugation is implied throughout the paper.
- [26] The sum runs over the selected jets. In the four-jets case, the first three leading jets are considered.
- [27] X. Portell, Ph.D. Thesis, U.A.B., Barcelona (2007).
- [28] G. De Lorenzo, Master Thesis, U.A.B., Barcelona (2008).
- [29] R. Cousins, Am. J. Phys. **63**, 398 (1995).
- [30] C. Albajar *et al.* (UA1 Collaboration), Phys. Lett. B **198**, 261 (1987); J. Alitti *et al.* (UA2 Collaboration), *ibid.* **B235**, 363 (1990).
- [31] LEPSUSYWG/02-06.2, <http://lepsusy.web.cern.ch/lepsusy/>.